

Assessing the Impact of Patient Lung Volume Variations on Absorbed Lung Doses at Y-90 Therapy Using GATE Toolkit

Ayşe Karadeniz Yıldırım ^{1,a,*}

¹ Opticians Programme, Vocational of Health Services, İstanbul Aydın University, İstanbul, Türkiye.

*Corresponding author

Research Article

History

Received: 05/12/2024

Accepted: 05/02/2025



This article is licensed under a Creative Commons Attribution-NonCommercial 4.0 International License (CC BY-NC 4.0)

ABSTRACT

In Y-90 treatment, the dose values received by the target organ and tumour, as well as the dose values received by critical organs, have a significant impact on the treatment planning process and ultimately determine the amount of activity to be used in the treatment. To this end, 10 different phantoms containing lung volumes ranging from small to large for the same activity values in the liver have been designed to evaluate the risk of lung toxicity in Y-90 treatment. Utilizing the GATE toolkit, a 10 mm diameter tumour volume containing 10 mCi activity has been positioned within the liver geometry, and the absorbed dose values have been calculated in lung volumes ranging from 3,103E+06 to 4,727E+06 mm³ in the right lung and from 2,021E+06 to 3,080E+06 mm³ in the left lung. Absorbed dose values have been calculated as maximum 3,046E-07±1,607E-08 Gy/s, minimum 1,868E-07±1,177E-08 Gy/s in left lung, maximum 8,772E-08±6,905E-09 Gy/s, minimum 5,164E-08±4,963E-09 Gy/s in right lung and maximum 3,923E-07±1,14852E-08 Gy/s, minimum 2,384E-07±8,36556E-09 Gy/s in total lung. The results of this study may indicate that the absorbed dose value in the lung increases with an increase in lung volume. A comparison has been made with existing studies in the literature.

Keywords: Lung dose, Lung volume, GATE MC, Dosimetry.

^a aysekaradeniz@aydin.edu.tr

^{id} <https://orcid.org/0000-0001-9301-4775>

Introduction

Yttrium-90 (Y-90) radioembolization, also known as selective internal radiation therapy (SIRT), has emerged as a leading treatment modality for liver-dominant cancers, such as hepatocellular carcinoma and metastatic colorectal cancer, particularly for patients who are not eligible for surgery or alternative forms of localized therapy [1-3]. Microspheres carrying the beta-emitting radioisotope Y-90 are inserted into the hepatic artery as part of this treatment (Fig.1). Once inside the tumor vasculature, the microspheres provide the cancer with targeted radiation. This targeted administration reduces the exposure of nearby healthy tissues while simultaneously improving the therapeutic efficacy within the liver. However, the nature of hepatic vasculature and the presence of potential arteriovenous shunts present a risk of microsphere migration to the lungs, resulting in unintended radiation exposure. This migration is quantified by the lung shunt fraction (LSF), which calculates the proportion of microspheres potentially reaching the pulmonary circulation [4,5]. Since too much radiation exposure to lung tissue can cause radiation pneumonitis or even pulmonary fibrosis, both of which have serious morbidities, it is imperative to estimate the absorbed dose to the lungs accurately.

The risk of radiation pneumonitis, a potentially serious side effect of excessive lung exposure, is strongly correlated with the lung dose absorbed, which is typically capped at 30 Gy for single-session exposures and 50 Gy for cumulative exposures in clinical guidelines [7,8] according to dosimetric studies in Y-90 radioembolization. However, individual anatomical variations, especially lung sizes,

which change radiation absorption and dose distribution throughout lung tissues, may not be adequately taken into account by these guidelines.

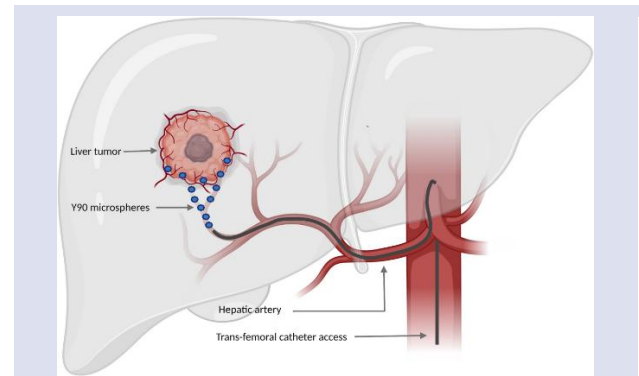


Figure 1. The visualization of Y-90 radioembolization [6].

Lung dosimetry in Y-90 treatment planning is guided by threshold limits that determine safe levels of absorbed dose [9] however, these limits may vary widely among individuals due to patient-specific anatomical differences, particularly lung volume. Variations in lung capacity affect how microspheres are distributed and retained, which changes the overall dose that is absorbed by the lung tissues [10]. For example, the absorbed dose per unit tissue may be lower in patients with higher lung capacities, which could minimize the risk of toxicity. Smaller lung capacities, on the other hand, might lead to a correspondingly higher absorbed dose, raising the risk of radiation-induced harm. However, existing dosimetry

models [11-13], which mainly concentrate on liver dosimetry without adequately accounting for patient-specific features in non-target organs like the lungs, frequently underrepresent these anatomical variances.

This study aims to address this gap by examining the impact of lung volume differences on the absorbed lung doses in patients undergoing Y-90 radioembolization. Our goal is to gain a better knowledge of how lung volumes can alter dose distribution through this study, which will help us improve risk assessment and individualized treatment planning for Y-90 therapy. Our objective is to improve clinical results by reducing the risk of lung toxicity

and guaranteeing safe yet efficient therapeutic radiation delivery to liver cancers by incorporating lung volume as a crucial component in dose modeling.

Material and Method

In this study, Y-90 radioembolization treatment, which is one of the radionuclide treatments applied in nuclear medicine clinics, was selected for internal dosimetry. It is established that the lung dose, liver parenchyma dose and tumour dose are determined by dosimetry [14]. Consequently, the geometry of these three tissues was incorporated into the study.

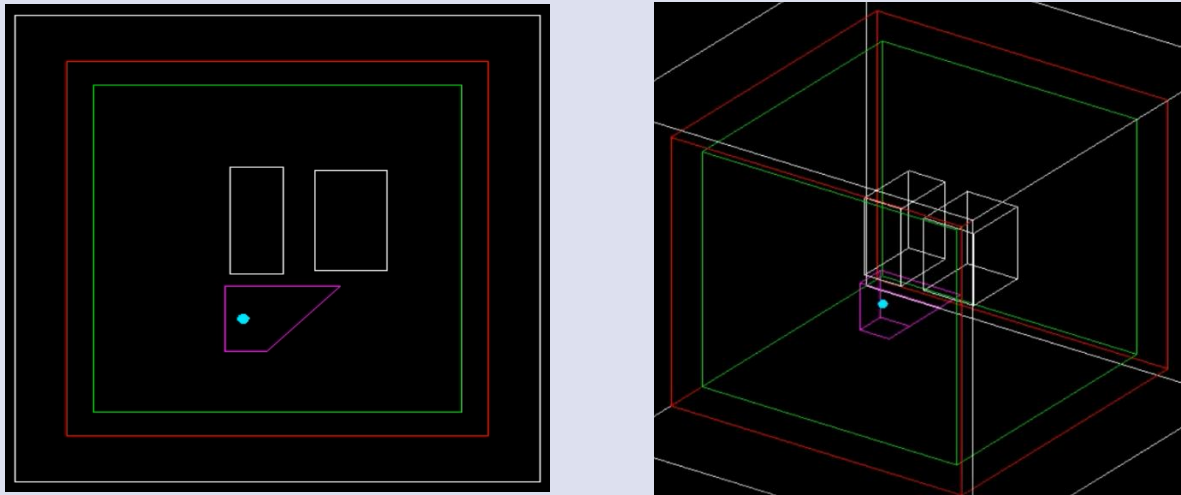


Figure 2. The visualization of virtual phantom geometry. In figures 2-a and 2-b, the lung is represented in white, the liver in magenta, and the tumor tissue in blue.

All Monte Carlo simulations were conducted on a computer with the macOS Monterey Version 12.6.3 operating system, a Core i5 2.7 GHz processor, 8 GB 1867 MHz DDR3 RAM and an Intel Iris 6100 graphics processor. The simulation process commenced with the generation of the phantom geometry in GATE version 8.1. The phantom geometry was designed to include the average volumes of the liver and lungs, and a spherical tumour with a radius of 10 mm was simulated in the liver. The geometry was created in a 700 mm³ cube filled with water. The dimensions of the liver are 220 mm, 140 mm and 80 mm in terms of length (x), height (y) and depth (z), respectively. The shapes of the left and right lungs were represented by rectangles with dimensions of (100 mm x

220 mm x 140 mm) and (137 mm x 230 mm x 150 mm), respectively. A visual representation of the geometry employed is presented in Figure 2.

The effects of lung volume differences on the absorbed lung doses in Y-90 radioembolization were quantitatively analyzed using simulations in the GATE toolkit. Patient-specific models with varying lung volumes were created. The dimensions of the right, left and total lung geometry [15] employed in the simulation are presented in Table 1. These include the width, length and depth in millimeters, as well as the volume in cubic millimeter and mass in kilograms.

Table 1. Size, volume and mass values of different lung volumes for which dose values were calculated in the simulation

	Left Lung				Right Lung				Total Lung	
	X[mm]	Y[mm]	Z[mm]	VL [mm3]	X[mm]	Y[mm]	Z[mm]	VR [mm3]	V [mm3]	m[kg]
1	80	261	135	3,080E+06	137	230	150	4,727E+06	7,807E+06	1,572
2	78	259	133	2,948E+06	135	228	147	4,525E+06	7,473E+06	1,500
3	76	257	131	2,820E+06	133	226	144	4,328E+06	7,148E+06	1,427
4	74	255	128	2,696E+06	131	224	141	4,138E+06	6,833E+06	1,351
5	72	253	126	2,575E+06	129	222	138	3,952E+06	6,527E+06	1,283
6	70	251	124	2,457E+06	127	220	135	3,772E+06	6,229E+06	1,260
7	68	249	122	2,343E+06	125	218	132	3,597E+06	5,940E+06	1,196
8	66	247	120	2,232E+06	123	216	129	3,427E+06	5,659E+06	1,134
9	64	245	118	2,125E+06	121	214	126	3,263E+06	5,388E+06	1,074
10	62	243	116	2,021E+06	119	212	123	3,103E+06	5,124E+06	1,016

The total lung volume used in the simulation was calculated to be between maximum 7,807E+06 m3 and minimum 5,124E+06 m3, between maximum 4,727E+06 m3 and minimum 3,103E+06 m3 for the right lung and between maximum 3,080E+06 m3 and minimum 2,021E+06 m3 for the left lung. Accordingly, lung mass values were calculated as a minimum of 1,016 kg and a maximum of 1,572 kg.

In the context of GATE simulations, the DoseActor is a sensitive detector with the capacity to store the energy present within its added volume and to interact with particle trace information. The DoseActor divides a given volume into three-dimensional voxels, which are then recorded with the associated event information. The volume-weighted algorithm employed by DoseActor entails the calculation of the actor's value by dividing the total energy stored within the defined volume by the total volume and density of the volume material. The dose distributions of all volumes were calculated in 1 mm sections along the y-axis using the C++ analysis code. The simulation was conducted independently for ten distinct lung volumes, as outlined in Table 1.

Table 2. Absorbed dose values and uncertainties at varying lung volumes and liver as a result of GATE MC simulation

	Lung Left Dose Value ± Uncertainty (Gy/s)	Lung Right Dose Value ± Uncertainty (Gy/s)	Total Lung Dose Value ± Uncertainty (Gy/s)
1	3,046E-07±1,607E-08	8,772E-08±6,905E-09	3,923E-07±1,14852E-08
2	2,900E-07±1,549E-08	8,238E-08±6,577E-09	3,724E-07±1,10322E-08
3	2,754E-07±1,503E-08	7,773E-08±6,271E-09	3,532E-07±1,06494E-08
4	2,614E-07±1,454E-08	7,299E-08±6,034E-09	3,344E-07±1,02878E-08
5	2,487E-07±1,412E-08	6,983E-08±5,962E-09	3,185E-07±1,00402E-08
6	2,333E-07±1,347E-08	6,617E-08±5,866E-09	2,995E-07±9,66976E-09
7	2,219E-07±1,310E-08	6,223E-08±5,594E-09	2,842E-07±9,34678E-09
8	2,091E-07±1,267E-08	5,840E-08±5,314E-09	2,675E-07±8,99114E-09
9	1,970E-07±1,212E-08	5,473E-08±5,112E-09	2,517E-07±8,61414E-09
10	1,868E-07±1,177E-08	5,164E-08±4,963E-09	2,384E-07±8,36556E-09

The dose values calculated in left, right and total lung volumes are given in Table 2, respectively. Absorbed dose values were calculated as maximum 3,046E-07±1,607E-08 Gy/s, minimum 1,868E-07±1,177E-08 Gy/s in left lung, maximum 8,772E-08±6,905E-09 Gy/s, minimum 5,164E-08±4,963E-09 Gy/s in right lung and maximum 3,923E-07±1,14852E-08 Gy/s, minimum 2,384E-07±8,36556E-09 Gy/s in total lung. The mean liver dose value for all lung volumes presented in Table 1 was determined to be 2,963E-03±2,024E-05 Gy/s.

Finally, electromagnetic interactions (photoelectric event, compton scattering, annihilation etc.) and radioactive decay processes were chosen to create physical processes in simulation. Mersenne Twister algorithm was used as a random number generator. The simulation was executed for a period of one second, utilizing a quantity of 10 mCi of Y-90. All macros were run consecutively for about 1 week to get all the data. The results were obtained as dose, uncertainty in dose, difference (percentage) in TXT file.

Results and Discussion

In the simulation, 10 different phantoms were designed with lung volumes ranging from small to large for an activity value of 10 mCi in the liver to assess the risk of lung toxicity in Y-90 treatment. Dose values and uncertainties in dose values were calculated for right, left and total lung volumes.

Given the anatomical proximity of the right lung to the liver, the absorbed dose value was measured with greater precision than that of the left lung.

The graph illustrating the relationship between right, left and total lung dose values and volume is presented in Figure 3. It can be observed that the absorbed dose values increase in line with an increase in volume.

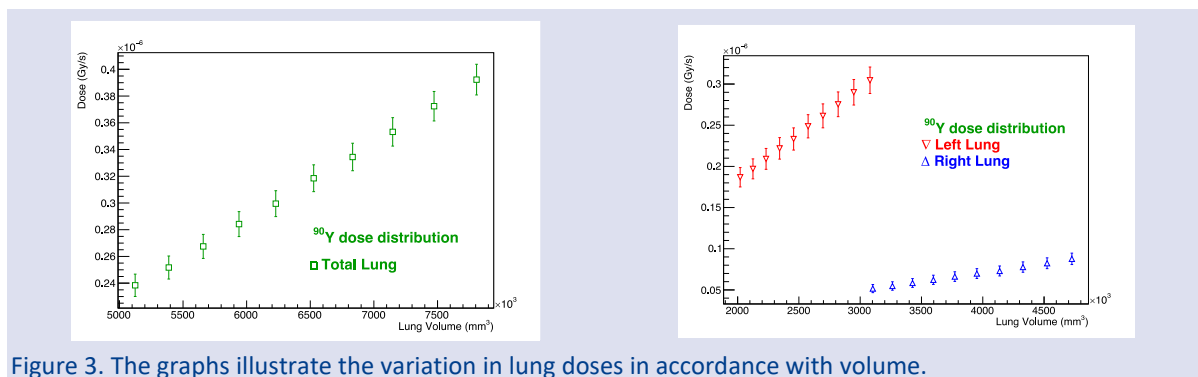


Figure 3. The graphs illustrate the variation in lung doses in accordance with volume.

In the calculation of critical and target organ doses in treatments involving Yttrium-90 radioembolization, the standard approach is to assume a lung mass of 1 kg [16-17]. In the literature, the mass of the lung is known to be 546 ± 207 g and 467 ± 174 g for women, 663 ± 239 g and 583 ± 216 g for men, including the right and left lung [18]. In the treatment of liver cancer, the doses received by organs such as the lung, which are considered critical, directly affect the treatment planning as well as the dose received by the target organ. In literature, it has been demonstrated that different volume values are obtained when various imaging techniques, including planar, SPECT/CT and PET/CT, are used to calculate lung and liver volumes. These differences have been known to have a significant impact on the determination of treatment doses [22, 23]. In this study, the potential risk of lung toxicity was assessed by modelling the impact of changes in lung volume on absorbed dose using Monte Carlo (MC) simulations. It was thus determined that an increase in lung volume resulted in an elevated dose absorption by the lung. In accordance with the findings of [24], when the discrepancies in lung volume were examined under an identical treatment plan, dose variations of up to 65% were observed between the lowest and highest volume values when the volume and dose data in Tables 1 and 2 were compared.

In the simulation, the calculated average absorbed dose value for a total lung volume of 7 litres was $3,726E-07\pm 1,106E-08$ Gy/s, while for 5 litres the value was $3,175E-07\pm 9,999E-09$ Gy/s and for 3 litres it was $2,604E-07\pm 8,829E-09$ Gy/s. This directly proportional relationship between lung volume and absorbed dose per unit volume indicates that larger lung volumes with the same vascularity are exposed to higher doses, which may increase radiation effects. The calculated dose differences for volumes of 3 to 5 litres and 5 to 7 litres were 22% and 17%, respectively. These findings are in agreement with this of previous study in [25], which emphasized a similar dose escalation in patients with larger lung volumes.

The findings of the study reinforce the crucial significance of lung volume in the evaluation of lung toxicity risk during Y-90 radioembolization. The results corroborate the conclusions of [20] that dosimetric models should incorporate anatomical variables such as lung volume to enhance the predictive precision of lung toxicity risk, underscoring that existing dosimetry protocols, which frequently fail to account for individual lung volume variations [10-13], are insufficient.

The results demonstrate the potential of utilizing simulation tools such as GATE to develop more personalized dosimetry models that account for lung volume differences [20, 26-30]. By incorporating patient-specific anatomy into dose calculations, GATE simulations can provide more accurate estimates of absorbed dose and, subsequently, guide safer treatment planning. Personalized models adjusting for lung volume, LSF and applied activity may enable practitioners to more accurately predict the risk of lung toxicity and, therefore, tailor the treatment plan accordingly.

While this study offers valuable insights into the relationship between lung volume and absorbed dose in Y-90 treatments, it is important to acknowledge the limitations of the study. It should be noted that the simulations presented in this study are based on generalized lung volumes, rather than patient-specific anatomical data. This may result in discrepancies when extrapolating the findings to a clinical setting. Furthermore, the shunt was assumed to have standardized vascularity, which inevitably affects the dose calculation. Further studies may benefit from the integration of real patient CT or MRI data, which could be used to refine lung dose estimates and improve the accuracy of dosimetry calculations. Furthermore, the longitudinal evaluation of post-treatment patients could confirm these findings by correlating simulated dose distributions with clinical outcomes of lung toxicity. The expansion of the range of anatomical variation and the investigation of different activity levels may also prove beneficial in optimizing dose thresholds for various patient populations.

Conclusion

This study shows that the amount of lung tissue that is absorbed during Y-90 therapy is significantly influenced by lung volume. The danger of radiation-induced lung damage increases with smaller lung capacities because they receive higher radiation doses per unit volume. Patients with different lung sizes may benefit from customized Y-90 treatments that optimize therapeutic efficacy while lowering toxicity risks by using the GATE toolkit for personalized dosimetry, which could enhance risk assessment.

Conflict of interest

There are no conflicts of interest in this work.

Acknowledgment

I would like to express my gratitude to Dr. Handan TANYILDIZI KÖKKÜLÜNK for her invaluable academic contribution to the research paper.

Ethical Approval Statement

No animals/humans were used for studies that are the basis of this research.

References

- [1] Kouri B.E., Abrams R.A., Al-Refaie W.B., et al., ACR appropriateness criteria radiologic management of hepatic malignancy, *J. Am. Coll. Radiol.*, 12(3) (2012) 265–273.
- [2] Ahmadzadehfar H., Biersack HJ., Ezziddin S., Radioembolization of liver tumors with yttrium-90 microspheres, *Semin Nucl Med*, 40 (2010) 105-21.
- [3] Mulcahy M.F., Lewandowski R.J., Ibrahim S.M., Sato K.T., Ryu R.K., Atassi B., Newman S., Talamonti M., Omary R.A., Benson A., Salem R., Radioembolization of colorectal hepatic metastases using yttrium-90 microspheres, *Cancer*, 115(9) (2009) 1849-58.

- [4] Covey A.M., Brody L.A., Maluccio M.A., Getrajdman G.I., Brown K.T., Variant hepatic arterial anatomy revisited: digital subtraction angiography performed in 600 patients, *Radiology*, 224(2) (2002) 542–547.
- [5] Lewandowski R.J., Sato K.T., Atassi B., et al., Radioembolization with 90Y microspheres: angiographic and technical considerations, *Cardiovasc. Intervent. Radiol.*, 30(4) (2007) 571–592.
- [6] Viñal D., Minaya-Bravo A., Prieto I. et al., Yttrium-90 transarterial radioembolization in patients with gastrointestinal malignancies, *Clin Transl Oncol*, 24 (2022) 796–808.
- [7] Harder E.M., Park H.S., Chen Z.J., Decker R.H., Pulmonary dose-volume predictors of radiation pneumonitis following stereotactic body radiation therapy, *Pract. Radiat. Oncol.*, 6 (2016) 353–359.
- [8] Yu N., Srinivas S.M., Difilippo F.P., Shrikanthan S., Levitin A., McLennan G., et al., Lung dose calculation with SPECT/CT for Yttrium-90 radioembolization of liver cancer, *Int J Radiat Oncol Biol Phys*, 85(3) (2013) 834–9.
- [9] Salem R., Johnson G.E., Kim E., Riaz A., Bishay V., Boucher E., Fowers K., Lewandowski R., Padia S.A., Yttrium-90 Radioembolization for the Treatment of Solitary, Unresectable HCC: The LEGACY Study, *Hepatology*, 74(5) (2021) 2342-2352.
- [10] Yuki B., Josep M., Takeo T., Sara L., Amita K., Pamela A., William S., Lucas F., Rahul S.P., Ganesh G., Edward K., Thomas D.S., Marcelo E. F., A comparative study of portal vein embolization versus radiation lobectomy with Yttrium-90 microspheres in preparation for liver resection for initially unresectable hepatocellular carcinoma, *Surgery*, 169(5) (2021) 1044-1051.
- [11] Smits M.L.J., Nijssen J.F.W., van den Bosch M.A.A.J., Lam M.G.E.H., Vente M.A.D., Huijbregts J.E., van het Schip A.D., Elschot M., Bult W., de Jong H.W.A.M., Meulenhoff P.C.W., Zonnenberg B.A., Holmium-166 radioembolization for the treatment of patients with liver metastases: design of the phase I HEPAR trial, *J. Exp. Clin. Cancer Res.*, 29 (2010) 70.
- [12] Bastiaannet, R., Kappadath, S.C., Kunnen, B., Braat A.J.A.T., Lam M.G.E.H., de Jong H.W.A.M., The physics of radioembolization, *EJNMMI Phys.*, 5(1) (2018) 22.
- [13] Gulec S.A., Mesoloras G., Stabin M., Dosimetric techniques in 90Y-microsphere therapy of liver cancer: The MIRD equations for dose calculations, *J. Nucl. Med.*, 47(7) (2006) 1209-1211.
- [14] Gulec S.A., Mesoloras G., Dezarn W.A., et al., Safety and efficacy of Y-90 microsphere treatment in patients with primary and metastatic liver cancer: the tumor selectivity of the treatment as a function of tumor to liver flow ratio, *J Transl Med.* 14 (2007) 5-15.
- [15] D'Angelis C. A., Coalson J. J., Ryan M.R., Pediatric critical care. Chapter 36-Structure of the respiratory system: lower respiratory tract, 4nd ed. Mosby, (2011) 490-498.
- [16] Margolis L.W., Philips T.L., Whole lung irradiation for metastatic tumour, *Radiology*, 93 (1969) 1173–8.
- [17] Stella M., van Rooij R., Lam M.G.E.H., de Jong H.W.A.M., Braat A.J.A.T., Lung Dose Measured on Postradioembolization ⁹⁰Y PET/CT and Incidence of Radiation Pneumonitis, *J Nucl Med.*, 63(7) (2022) 1075-1080.
- [18] Grandmaison G.L., Clairand I., Durigon M., Organ weight in 684 adult autopsies: new tables for a Caucasoid population, *Forensic Science International*, 119(2) (2001) 149-154.
- [19] Elsayed M., Cheng B., Xing M., et al., Comparison of Tc-99m MAA Planar Versus SPECT/CT Imaging for Lung Shunt Fraction Evaluation Prior to Y-90 Radioembolization: Are We Overestimating Lung Shunt Fraction?, *Cardiovasc Intervent Radiol*, 44 (2021) 254–260.
- [20] Gill H., Hiller J., Systematic review of lung shunt fraction quantification comparing SPECT/CT and planar scintigraphy for yttrium 90 radioembolization planning, *Clin Transl Imaging*, 9 (2021) 181–188.
- [21] Mercolli L., Zeimpekis K., Prenosil G.A., Sari H., Rathke H.G., Rominger A., Shi K., Phantom study for ⁹⁰Y liver radioembolization dosimetry with a long axial field-of-view PET/CT, *Phys Med.*, 118 (2024) 103296.
- [22] Allred J.D., Niedbala J., Mikell J.K., et al., The value of ^{99m}Tc-MAA SPECT/CT for lung shunt estimation in ⁹⁰Y radioembolization: a phantom and patient study, *EJNMMI Res* 8, 50 (2018).
- [23] D'Arienzo M., Pimpinella M., Capogni M., et al., Phantom validation of quantitative Y-90 PET/CT-based dosimetry in liver radioembolization, *EJNMMI Res* 7, 94 (2017).
- [24] Busse N., Erwin W., Pan T., Evaluation of a semiautomated lung mass calculation technique for internal dosimetry applications, *Med Phys.*, 40(12) (2013) 122503.
- [25] Georgiou M.F., Kuker R.A., Studenski M.T., et al., Lung shunt fraction calculation using ^{99m}Tc-MAA SPECT/CT imaging for ⁹⁰Y microsphere selective internal radiation therapy of liver tumors. *EJNMMI Res* 11, 96 (2021).
- [26] Karimipourfard M., Sina S., Alavi M.S, Toward three-dimensional patient-specific internal dosimetry using GATE Monte Carlo technique, *Radiation Physics and Chemistry*, 95 (2022) 110046.
- [27] Arun G., et al., Preclinical voxel-based dosimetry through GATE Monte Carlo simulation using PET/CT imaging of mice, *Physics in Medicine and Biology*, 64(9) (2019) 095007.
- [28] Tanyıldızı- Kokkulunk H., Demir M., Karadeniz-Yildirim A., Ozkorucuklu S., Doğan Y., Akkuş B., Y-90 Dosimetry with Monte Carlo Method: GATE Validation with STL Formatted Phantom, *ACTA PHYSICA POLONICA A*, 138(6) (2020) 801-808.
- [29] Karadeniz-Yildirim A., Ozkorucuklu S., Tanyildizi-Kokkulunk H. et al., Monte Carlo Simulation of Liver Dosimetry with Yttrium-90 Radionuclide Using Gate: 3D Phantom, *Bull. Lebedev Phys. Inst*, 51 (2024) 30–37.
- [30] Karadeniz-Yildirim A., Tanyildizi-Kokkulunk H., Comparison of Y-90 and Ho-166 Dosimetry Using Liver Phantom: A Monte Carlo Study, *Anti-Cancer Agents in Medicinal Chemistry (Formerly Current Medicinal Chemistry - Anti-Cancer Agents)*, 22(7) (2022) 1348-1353.